A Simple and Efficient Tool for Design Analysis of Synchronous Reluctance Motor

Tahar Hamiti, Thierry Lubin, and Abderrezak Rezzoug

Groupe de Recherche en Electrotechnique et Electronique de Nancy, Université Henri Poincaré 54506 Nancy, France

We present an efficient tool for design analysis of a synchronous reluctance motor (SynRM). We use winding function analysis (WFA) instead of finite-element analysis (FEA). With WFA, parameter sensitivity can be analyzed and the effects of parameters on the machine design can be evaluated very rapidly (under linear condition). We investigated the effect of rotor skewing, stator winding chording, pole arc, and interpolar air-gap length on average torque and torque ripple. We compare the results obtained by WFA with those obtained by 2-D FEA. We show that the two methods give approximately the same results but WFA requires less computation time.

***Index Terms*—Finite-element method, reluctance motor, torque ripple, winding function.**

NOMENCLATURE

R	Rotor outer radius (m).
L	Active axial length (m).
Ne	Number of stator slots.
W	Number of turns in series per phase.
α	Angular position along the stator inner surface (rad).
θ	Electrical angular position of the rotor (rad).
$e_s(\theta)$	Stator air-gap length function (m).
$e_r(\alpha-\theta)$	Rotor air-gap length function (m).
i_a, i_b, i_c	Currents of phase a, b, and c, respectively (A).
L_a, L_b, L_c	Self inductance of phase a, b, and c (H).
L_{ab}, L_{ab}, L_{bc}	Mutual inductances (H).
Γ	Instantaneous torque (N.m).
$\Gamma_{\rm avg}$	Average torque (N.m).
$\Delta\Gamma$	Torque ripple (%).
$e1$	Air-gap length (mm).
$e2$	Interpolar air-gap length (mm).
β	Pole arc (degree).
δ	Skewing angle (degree).
k	Chording factor.

Digital Object Identifier 10.1109/TMAG.2008.2004536

Color versions of one or more of the figures in this paper are available online at http://ieeexplore.ieee.org.

I. INTRODUCTION

THE synchronous reluctance motor (SynRM) is an interesting solution for variable frequency drives and servomechanisms [1], [2]. In its cut-out rotor version, despite poor efficiency and power factor, its cost manufacturing, ruggedness, and synchronism with power supply frequency can constitute a good challenge, while an optimal design for maximum torque and minimum torque ripple must be achieved. To maximize average torque and power factor of a line-start SynRM, an analytical design model is proposed in [3]. However, it does not take into account torque ripple which is a serious drawback especially when position control is needed. Furthermore, the motor was designed for self-starting operation, thus it contains a squirrel cage which adds an other constraint for the design task, and is subject to additional losses. Vector control permits synchronous self starting without damping bars.

Bomela and Maarten have done a study on stator chording and rotor skewing effect on average torque, power factor and torque ripple [4]. This study has been evaluated by finite-element analysis (FEA) which is, as known, very time consuming. Broadly, very much attention is given for high anisotropy normally or axially laminated flux barrier SynRM [5], [6]. With this type of structure, high performance drives can be achieved but manufacturing simplicity is lost.

We have shown in [7] that accurate shapes of inductances and electromechanical torque can be obtained using the winding function theory. The computation quickness of this method constitutes its main advantage when several stator and rotor geometries are to be tested, also when a refined model of the machine must be inserted within a complex simulation control scheme.

This paper proposes a use of winding function analysis to design an optimized SynRM in terms of average torque and torque ripple. The cross section of the stator and the rotor structure of the studied SynRM is shown in Fig. 1. The rotor presents a simple and robust structure without damper bars. The stator is the same as the one of an induction machine and has three-phase distributed winding within 36 slots. The machine dimension details are given in Table I.

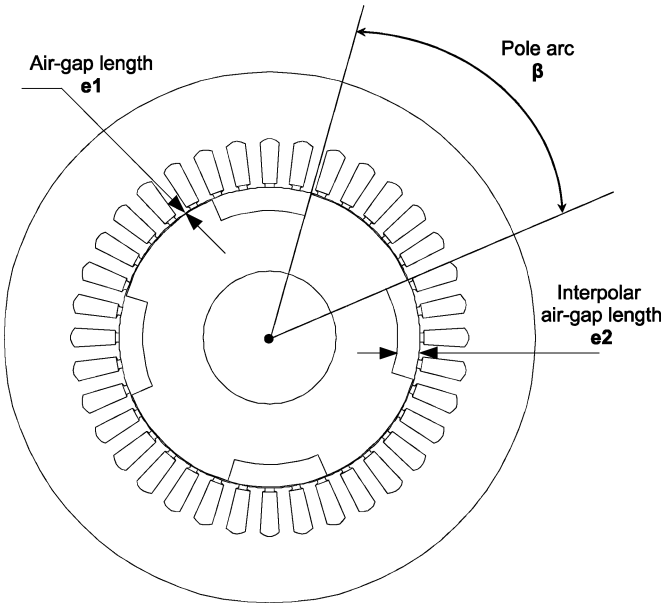

Fig. 1. Cross section of the studied SynRM.

TABLE I
DIMENSIONS OF THE MACHINE

Symbol	Quantity	Value
P	Number of pole pairs	2
R	Rotor outer radius	45 mm
e_1	Air-gap length	0.26 mm
W	Number of turns/slot	29
Ne	Number of stator slots	36
L	Active axial length	155 mm
β	Pole arc	Variable
e2	Interpolar air-gap length	Variable
δ	Skewing angle	Variable
k	Chording factor	Variable

II. COMPUTATION PROCEDURE AND RESULTS

A. Winding Function Analysis (WFA)

Winding function theory [8] gives the self and mutual inductances expression as

$$L_{ij} = \mu_0 RL \int_0^{2\pi} \frac{1}{e_s(\theta) + e_r(\alpha - \theta)} N_i(\alpha) N_j(\alpha) d\alpha. \quad (1)$$

In this expression, $N_i(\alpha)$ is called the winding function i and represents in fact the magnetomotive force distribution along the air-gap per unit current flowing in the stator winding i. The rotor and stator air-gap length functions $e_r(\alpha-\theta)$ and $e_s(\alpha)$ of the studied SynRM have been defined in [7].

The instantaneous torque computation is obtained by

$$\Gamma = \frac{1}{2}[\mathbf{I}]^t \left[\frac{\partial \mathbf{L}}{\partial \theta}\right][\mathbf{I}] \quad (2)$$

with

$$[\mathbf{L}] = \begin{bmatrix} L_a(\theta) & L_{ab}(\theta) & L_{ac}(\theta) \\ L_{ab}(\theta) & L_b(\theta) & L_{bc}(\theta) \\ L_{ac}(\theta) & L_{bc}(\theta) & L_c(\theta) \end{bmatrix} \quad (3)$$

and

$$[\mathbf{I}] = \begin{bmatrix} i_a(\theta) \\ i_b(\theta) \\ i_c(\theta) \end{bmatrix}. \quad (4)$$

For a given structure of the machine, (1) is numerically integrated after the definition of winding and air-gap functions [7]. For each rotor position, (2) is computed with the following imposed currents:

$$\begin{aligned} i_a &= \sqrt{2} I_{\text{rms}} \cos(\theta + \phi); \\ i_b &= \sqrt{2} I_{\text{rms}} \cos\left(\theta - \frac{2\pi}{3} + \phi\right) \\ i_c &= \sqrt{2} I_{\text{rms}} \cos\left(\theta + \frac{2\pi}{3} + \phi\right). \end{aligned} \quad (5)$$

To avoid saturation I_{rms} is fixed to $2A$ and the electrical current phase ϕ is fixed to 45° in order to develop the maximum average torque.

B. Study of Parameter Sensitivity

To minimize the ratio of the torque ripple $\Delta\Gamma$ to the average torque Γ_{avg}, the skewing angle δ, the chording factor k, the pole arc β and the interpolar air-gap length $e2$ have to be considered (Table I).

Every parameter influence is studied by calculating

$$\Gamma_{\text{avg}} = \frac{1}{N_p} \sum_{i=1}^{N_p} \Gamma(i) \quad (6)$$

$$\Delta\Gamma = \frac{\max(\Gamma) - \min(\Gamma)}{\Gamma_{\text{avg}}}. \quad (7)$$

Np is the number of points over one computation period. 3600 points ensures a satisfying precision.

1) Effect of Rotor Skewing (δ): To reduce the ripple torque caused by the slots, the well known technique is the skewing.

To simulate the 3-D effect generated by the skewing, multiple 2-D unskewed submachines are considered as shown in Fig. 2 [9]. With WFA, thanks to the refined path resolution ($Np = 3600$), computing only the average value over N_s points of the unskewed inductances, we obtain the skewed inductances as

$$L_{sk_i} = \frac{1}{N_s} \sum_{r=-\frac{N_s}{2}}^{-\frac{N_s}{2}} L_i(r) \quad (8)$$

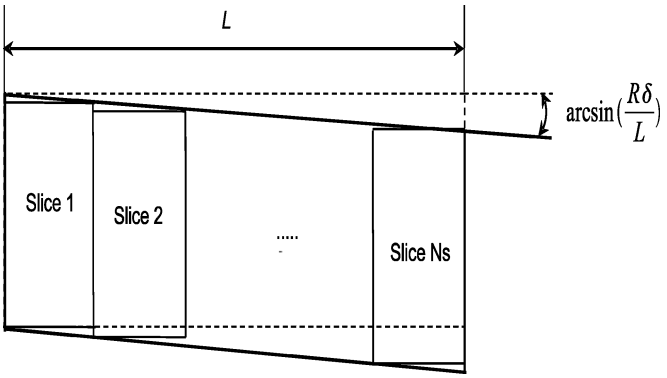

Fig. 2. Axial view of the skewed rotor.

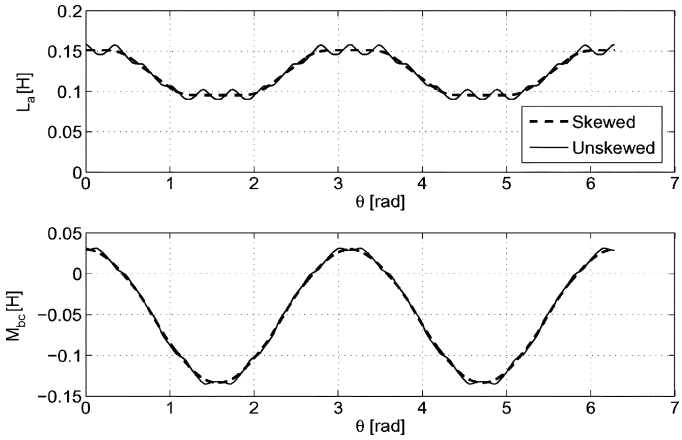

Fig. 3. Self- and mutual- skewed ($\delta = 10°$) inductances, with $\beta = 0.5$, $e2 = 10$ mm, not chorded winding, skewed rotor.

$$M_{sk_ij} = \frac{1}{N_s} \sum_{r=-\frac{N_s}{2}}^{-\frac{N_s}{2}} M_i(r) \tag{9}$$

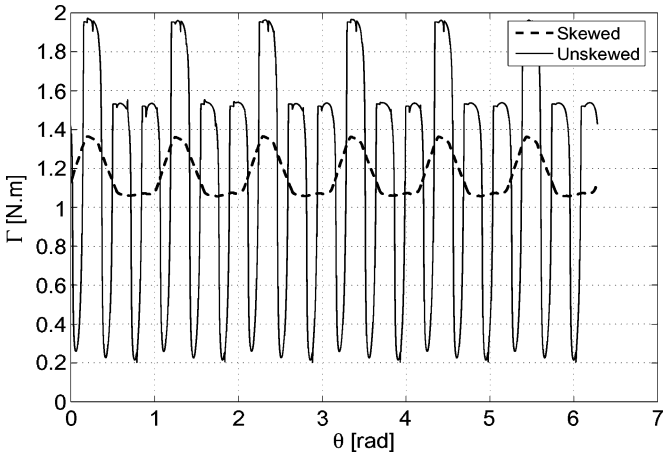

Fig. 4. Torque of skewed ($\delta = 10°$) and unskewed machine.

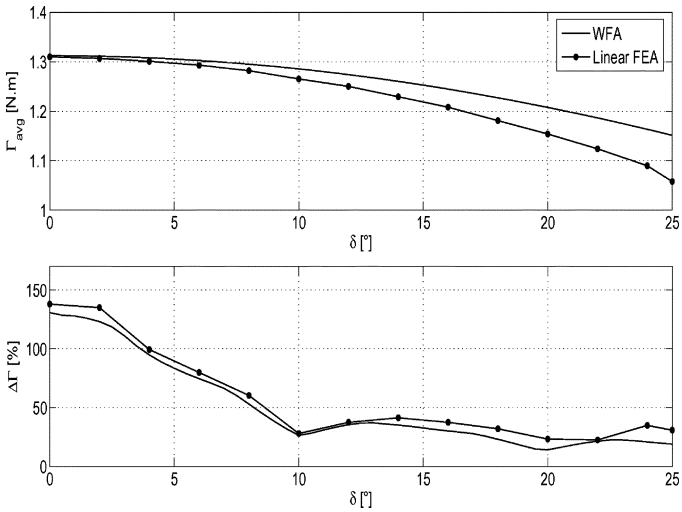

Fig. 5. Average torque and torque ripple versus skewing angle.

where N_s is the integer number of the skewing angle/path resolution (0.1°) ratio. After computing (8) and (9), the torque is obtained by (2). With FEA software [10], because of the required time computation, the path angle resolution is 1°, we cannot obtain the skewed torque by averaging. Hence, to compute correctly, the skewed torque, 10 slices must be taken.

Figs. 3 and 4 show the inductances and the instantaneous torque for unskewed and one slot pitch (10°) skewed rotor. Differently than flux barrier rotor SynRL [5], the salient-pole SynRL becomes free of slots ripple torque with exactly a full stator slot pitch. The residual torque ripple is due to the distributed winding and the rotor saliency.

The influence of the skewing angle on both average and ripple torque is shown in Fig. 5. It illustrates the optimum skewing angle ($\delta = 10°$) that is pointed on above. In this case we denote a reduction of torque ripple from 130% up to 26% and a decrease of average torque by only 3%.

2) Effect of Stator Winding Chording (k): The effect of stator winding chording on the torque ripple and average torque is investigated by varying the fractional pitch windings. Fig. 6 represents the winding functions of the phase "a" in the cases of full pitch winding and 7/9 chorded winding. It has been shown in [4] that chording the stator of a flux barrier SynRL has very little effect on the torque ripple. That is false in our case. Indeed, Fig. 7 shows an important reduction of torque ripple without a sensitive drop on the average torque for a chording factor of 8/9 whatever β.

3) Effect of the Pole Arc (β): The saliency angle is a deterministic parameter for a cut-out rotor SynRM. In [3], an optimum angle of 45° was found. However, no attention has been given to the influence of this parameter on torque ripple. Fig. 8 shows the effect of the pole arc (β) on both the average and ripple torque. The optimum β for maximum average torque is 43° and for minimum torque ripple is 44°. With FEA, the optimum angle is 40° for both ripple and average torque. However, we can observe that the curves are relatively flat in the interval [40°, 45°], and we can thus choose an angle within this interval. It is important to note that even not 1 minute is required to compute the whole skewed torque with WFA against more than 2 hours with FEA.

4) Effect of the Interpolar Gap Length ($e2$): The interpolar gap length has been defined in Fig. 1. Its influence is also studied and the results are shown in Fig. 9. We can observe that beyond the value of approximately 20 for the ratio $e2/e1$ the average

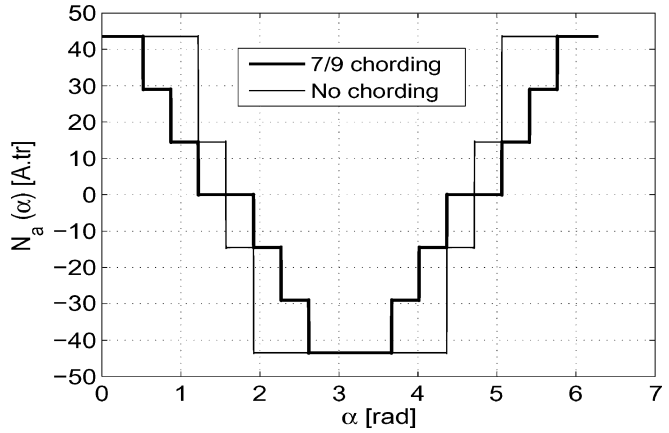

Fig. 6. No chorded and 7/9 chorded winding function of the phase "a".

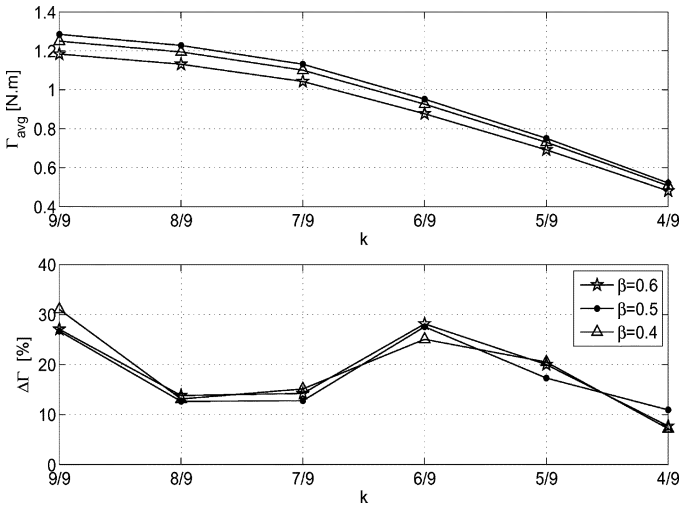

Fig. 7. Average torque and torque ripple versus chording factor of the skewed ($\delta = 10°$) machine.

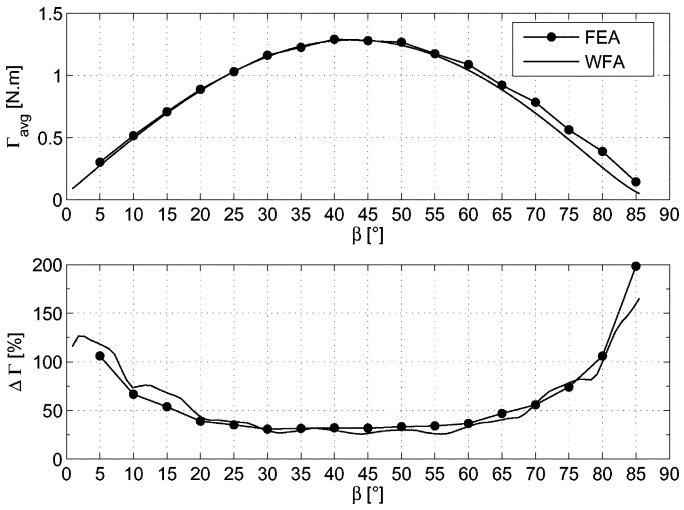

Fig. 8. Average torque and torque ripple versus β of the skewed ($\delta = 10°$) machine.

and ripple torque are not subject to sensitive variation. Moreover, this low value is beneficial for mechanical ruggedness and

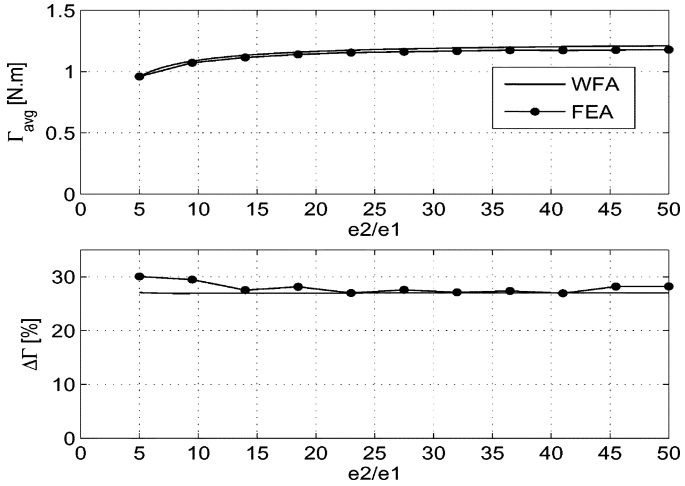

Fig. 9. Average torque and torque ripple versus interpolar gap length $e2$ to air-gap length $e1$ ratio of the skewed ($\delta = 10°$) machine.

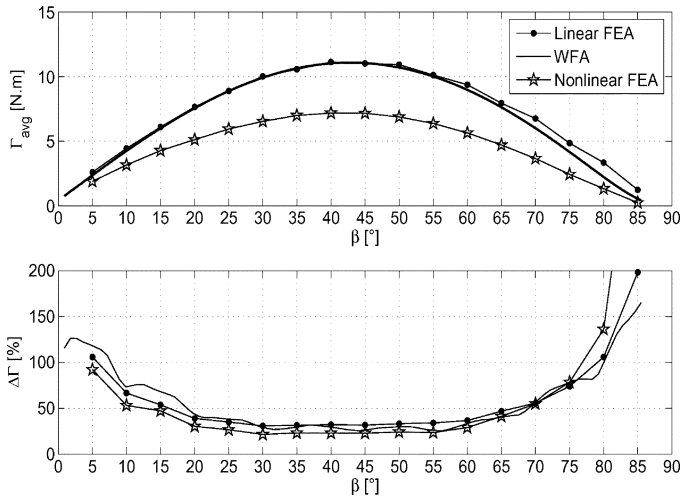

Fig. 10. Average torque and torque ripple versus β of the skewed ($\delta = 10°$) machine.

for a judicious choice of rotor yoke length to avoid flux path undersizing.

III. Effect of the Magnetic Saturation

In order to check if the magnetic saturation has an influence on the optimized parameters obtained by WFA, FEA is used by considering a nonlinear magnetic $B(H)$ characteristic and an $I_{\rm rms}$ value of $6A$. Fig. 10 shows the superposed results of the two methods and leads to the following observations. Firstly, the optimum pole arc stay the same for both linear and nonlinear cases. Secondly, as commonly known, the average produced torque is strongly decreased by the saturation.

IV. Prototype Realization

The prototype reluctance motor is designed on the basis of a standard 4-pole, 3-kW squirrel cage induction motor. The stator of the considered motor contains 36 slots with three-phase full pitch winding ($k = 9/9$). The skewing angle of the rotor bars

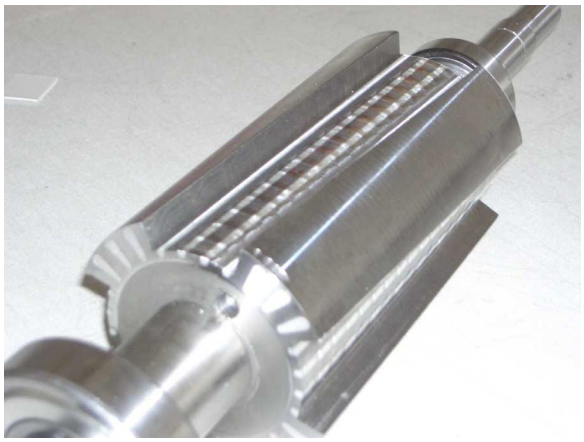

Fig. 11. Photography of the prototype rotor.

being equal to 13° determines the direction of milling to obtain the rotor salient poles. The manufactured rotor is shown in Fig. 11. It has the following parameters: $\beta = 45°$, $e2 = 10\,\mathrm{mm}$, and $\delta = 13°$. To avoid damping effect, the rotor end-rings are cut off. As demonstrated previously, the best values of the chording factor k and skewing angle δ are respectively 8/9 and 10°. One can observe in Fig. 5 that the curve representing the torque ripple versus δ is relatively flat between $\delta = 10°$ and $\delta = 15°$, so the chosen skewing angle is suitable to verify the theory. To investigate the chording effects on the torque ripple, in addition to the original stator with $k = 9/9$, another one having $k = 8/9$ is currently under construction. Experimental tests will be done in future work in order to validate the theoretical results.

V. Conclusion

An entire study of a four-pole, 36-slot, three-phase SynRM is done with a simple and fast computation method based on winding function theory. The improvement of the method is verified with finite-element analysis. It is shown that to obtain minimum torque ripple and maximum average torque, the rotor must be skewed by a stator slot pitch, a chording factor of 8/9 ensures a good compromise, it is not necessary to have a very large interpolar air-gap length (a value of 20 times $e1$ is sufficient), and the optimal pole arc is around 45°. An optimized rotor prototype has been manufactured by milling the one of an existing induction machine. Future work consists of experimental validation of the theoretical results.

Furthermore, as the proposed method is not time consuming, it can be easily used within a global design optimization task. For that, one can use for example genetic algorithms or sequential quadratic programming.

References

[1] I. Boldea, *Reluctance Synchronous Machines and Drives*. Oxford, U.K.: Clarendon/Oxford, 1996.

[2] A. Vagati, "The synchronous reluctance solution: A new alternative in A.C. drives," in *Proc. Int. Conf. Ind. Electron. Contr. Instrumentation*, 1994, pp. 1–13.

[3] I. B. Chabu, J. R. Cardoso, V. C. Silva, S. I. Nabeta, and A. Foggia, "A new design technique based on a suitable choice of rotor geometrical parameters to maximise torque and power factor in synchronous reluctance motors: Part I and II," *IEEE Trans. Energy Convers.*, vol. 14, no. 3, pp. 599–609, 1997.

[4] X. B. Bomela and M. J. Kamper, "Effect of stator chording and rotor skewing on performance of reluctance synchronous machine," *IEEE Trans. Ind. Appl.*, vol. 38, no. 1, pp. 91–100, 2002.

[5] A. Vagati, M. Pastorelli, G. Franceschini, and S. C. Petrache, "Design of low-torque-ripple synchronous reluctance motors," *IEEE Trans. Ind. Appl.*, vol. 34, no. 4, pp. 758–765, 1998.

[6] T. J. E. Miller, A. Hutton, C. Cossar, and D. Staton, "Design of a synchronous reluctance motor dive," *IEEE Trans. Ind. Appl.*, vol. 27, no. 4, pp. 741–749, 1991.

[7] T. Lubin, T. Hamiti, H. Razik, and A. Rezzoug, "Comparison between finite element analysis and winding function theory for inductances and torque calculation of a SynRM," *IEEE Trans. Magn.*, vol. 43, no. 8, pp. 3406–3410, Aug. 2007.

[8] I. Tabatabaei, J. Faiz, H. Lesani, and M. T. Nabavi-Razavi, "Modeling and simulation of a salient-pole synchronous generator with dynamic eccentricity using modified winding function theory," *IEEE Trans. Magn.*, vol. 40, no. 3, pp. 1550–1555, May 2004.

[9] J. F. Eastham, D. M. Ionel, M. J. Balchin, and T. Betzer, "Finite element analysis of an interior-magnet brushless D.C. machine, with a step-skewed rotor," *IEEE Trans. Magn.*, vol. 33, no. 2, pp. 2117–2119, Mar. 1997.

[10] D. C. Meeker, Finite Element Method Magnetics ver. 4.0, Jun. 17, 2004 [Online]. Available: http://femm.foster-miller.net

Manuscript received October 07, 2007; revised August 04, 2008. Current version published January 08, 2009. Corresponding author: T. Lubin (e-mail: thierry.lubin@green.uhp-nancy.fr).

Tahar Hamiti was born in Larbàa Nath Irathen, Algeria, in 1979. He received the M.Sc. degree from the University of Nancy, Nancy, France, in 2003. He is currently pursuing the Ph.D degree.

His research interests include reluctance machines, modeling, and control.

Tierry Lubin was born in Sedan, France, in 1970. He received the M.Sc. degree from the University of Paris 6, Paris, France, in 1994 and the Ph.D. degree from the University of Nancy, Nancy, France, in 2003.

He is currently a Lecturer with the University of Nancy. His interests include electrical machines, modeling, and control.

Abderrezak Rezzoug is a Professor in electrical engineering at the University Henri Poincaré, Nancy, France. He is currently the Dean of the Groupe de Recherche en Electrotechnique et Electronique de Nancy.His main subjects of research concern electrical machines, their identification, diagnostics and control, and superconducting applications.